AFRL-RH-WP-TR-2012-0087

Detection of Orexin A Neuropeptide in Biological Fluids Using a Zinc Oxide Field Effect Transistor

Joshua Hagen, Wanda Lyon, Yaroslav Chushak, Morley Stone, Nancy Kelley-Loughnane

Human Performance Wing
Human Effectiveness Directorate

Melanie Tomczak, Rajesh Naik

Materials and Manufacturing Directorate

JUNE 2012
Final Report

AIR FORCE RESEARCH LABORATORY
711TH HUMAN PERFORMANCE WING,
HUMAN EFFECTIVENESS DIRECTORATE,
WRIGHT-PATTERSON AIR FORCE BASE, OH 45433
AIR FORCE MATERIEL COMMAND
UNITED STATES AIR FORCE

NOTICE AND SIGNATURE PAGE

Using Government drawings, specifications, or other data included in this document for any purpose other than Government procurement does not in any way obligate the U.S. Government. The fact that the Government formulated or supplied the drawings, specifications, or other data does not license the holder or any other person or corporation; or convey any rights or permission to manufacture, use, or sell any patented invention that may relate to them.

This report was cleared for public release by the 88th Air Base Wing Public Affairs Office and is available to the general public, including foreign nationals. Copies may be obtained from the Defense Technical Information Center (DTIC) (http://www.dtic.mil).

AFRL-RH-WP-TR-2012-0087 HAS BEEN REVIEWED AND IS APPROVED FOR PUBLICATION IN ACCORDANCE WITH ASSIGNED DISTRIBUTION STATEMENT.

//signature//

Nancy Kelley-Loughnane, Work Unit Manager
Human Signatures Branch

//signature//

LOUISE A. CARTER, Chief
Forecast Division
Human Effectiveness Directorate
711th Human Performance Wing
Air Force Research Laboratory

This report is published in the interest of scientific and technical information exchange, and its publication does not constitute the Government's approval or disapproval of its ideas or findings.

REPORT DOCUMENTATION PAGE

Form Approved
OMB No. 0704-0188

1. REPORT DATE *(DD-MM-YY)*	2. REPORT TYPE	3. DATES COVERED *(From - To)*
15 06 12	Final	26 Jan 2010 – 30 Jun 2012

4. TITLE AND SUBTITLE

Detection of Orexin A Neuropeptide in Biological Fluids Using a Zinc Oxide Field Effect Transistor

5a. CONTRACT NUMBER
In-House

5b. GRANT NUMBER

5c. PROGRAM ELEMENT NUMBER
62202F

6. AUTHOR(S)
Joshua Hagen*, Wanda Lyon*, Yaroslav Chushak*, Melanie Tomczak**, Rajesh Naik**, Morley Stone*, Nancy Kelley-Loughnane*

5d. PROJECT NUMBER
7184

5e. TASK NUMBER
C

5f. WORK UNIT NUMBER
7184C001

7. PERFORMING ORGANIZATION NAME(S) AND ADDRESS(ES)
**Materials and Manufacturing Directorate
Air Force Research Labs
Wright Patterson Air Force Base, Dayton OH

8. PERFORMING ORGANIZATION REPORT NUMBER

9. SPONSORING/MONITORING AGENCY NAME(S) AND ADDRESS(ES)
*Air Force Materiel Command
Air Force Research Laboratory
711th Human Performance Wing
Human Effectiveness Directorate
Forecasting Division
Human Signatures Branch
Wright-Patterson AFB, OH 45433

10. SPONSORING/MONITORING AGENCY ACRONYM(S)
711 HPW//RHXB

11. SPONSORING/MONITORING AGENCY REPORT NUMBER(S)
AFRL-RH-WP-TR-2012-0087

12. DISTRIBUTION/AVAILABILITY STATEMENT
Distribution A: Approved for public release; distribution unlimited.

13. SUPPLEMENTARY NOTES
88ABW-2012-2072, cleared 6 April 2012

14. ABSTRACT

Biomarkers which are indicative of acute physiological and emotional states are studied in a number of different areas in cognitive neuroscience. Currently, many cognitive studies are conducted based on programmed tasks followed by timed biofluid sampling, central lab processing, and followed by data analysis. In this work, we present a sensor platform capable of real-time biomarker detection specific for detecting neuropeptide orexin A, found in blood and saliva and known as an indicator of fatigue and cognitive performance. A peptide recognition element that selectively binds to orexin A was designed, characterized, and functionalized onto a zinc oxide field effect transistor to enable real-time detection. The detection limit using the sensor platform was 100 aM in water, and fM-nM levels in saliva and serum, respectively. The transistor and recognition element sensor platform can be easily expanded allowing for multiple biomarkers to be detected simultaneously, lending itself to complex biomarker analysis applicable to real-time feedback for neuroscience research and physiological monitoring.

15. SUBJECT TERMS
Biomarkers, Orexin A, Cellular Engineering, Circuits, Nanotechnology, Photonics, Field Effect Transistor

16. SECURITY CLASSIFICATION OF:			17. LIMITATION OF ABSTRACT:	18. NUMBER OF PAGES	19a. NAME OF RESPONSIBLE PERSON (Monitor)
a. REPORT	b. ABSTRACT	c. THIS PAGE			Nancy Kelley-Loughnane
Unclassified	Unclassified	Unclassified	SAR	39	19b. TELEPHONE NUMBER *(Include Area Code)* N/A

Standard Form 298 (Rev. 8-98)
Prescribed by ANSI Std. Z39-18

THIS PAGE IS INTENTIONALLY LEFT BLANK

TABLE OF CONTENTS

LIST OF FIGURES

AUTHOR CONTRIBUTIONS

J.H. designed, tested, and analyzed the PeptiFETs, W.L. identified the orexin A binding peptide through phage display and characterized binding kinetics, Y.C. designed, tested, and analyzed all modeling data, M.T. identified the ZnO binding peptide and designed the fusion peptides, , J.H, W.L, and Y.C. wrote the manuscript, R.N., M.S., N.K.L. provided ideation, direction, and data/results discussion.

ACKNOWLEGEMENTS

We are grateful to B. Bayraktaroglu and K. Leedy of the Sensors Directorate for fabrication of zinc oxide FETs, S.N. Kim for valuable discussions and expertise in sensor testing, J.L. Chavez for continued helpful discussions, L. Narayanan for HPLC analysis, J. Schlager for support in BRE identification. This work was supported by the Air Force Research Laboratory, Bio-X Strategic Technology Team, 711th Chief Scientist Seedling Fund, and BSEM program in the Materials and Manufacturing Directorate.

COMPETING INTERESTS STATEMENT

The authors declare that they have no competing financial interests.

1.0 INTRODUCTION

The distribution of orexin peptides and their receptors in the brain suggests that they may play a key role in multiple regulatory systems, including feeding, autonomic control, sleep, memory, and the reward system (for recent review see[1]). Experiments revealed that orexin levels in the lateral hypothalamic area of rats gradually increased during the active period and exponentially declined in the rest phase[2]. The levels of orexin A in the cerebrospinal fluid[3] or plasma[4] of narcoleptic patients is abnormally decreased (reduction 80 to 100%). Additionally, a correlation between orexin A levels and individuals with post traumatic stress disorder (PTSD) was made where the level was noticeably decreased[5]. There is a considerable amount of evidence suggesting a regulatory role of orexin peptides in cognition performance impaired by sleep deprivation. It was found that intranasal application of orexin A reduces the effect of sleep deprivation on the cognitive performance in non-human primates[6]. On the other hand, the administration of an orexin-1 receptor antagonist decreased the attentional performance in rats[7], suggesting that orexins contribute to the attention. Therefore, it is hypothesized that measuring the level of orexin A in blood of human subjects can allow us to predict a vigilance state and cognitive performance. Orexin A and B are both produced from a common precursor polypeptide by proteolytic cleavage. The sequences of orexin A are completely conserved among several mammalian species while orexin B is highly conserved (93%) with two residues substituted in rat and mouse comparing with the human sequence[8]. Human orexin A neuropeptide has 33 amino acids and contains two disulfide bonds in N-terminal region. The concentration of orexin A in tissue and blood is much higher than the concentration of orexin B, where orexin A can be found at pg/mL levels, and orexin B is undetectable[9]. Furthermore, orexin A is highly lipophilic and can rapidly cross the blood-brain barrier[10]. In contrast, orexin B has low lipophilicity and is rapidly metabolized in blood which makes it difficult to detect. Orexin neuropeptides act via two G protein-coupled cell surface receptors named orexin receptor-1 (Ox1R) and orexin receptor two (Ox2R). The activation of Ox1R by orexin A is 10 to 100 times higher than that of orexin B, whereas the activity at the Ox2R is in the same range for both peptides[11].

Current techniques for measuring orexin A levels in blood and saliva require fluid sampling and transportation to a laboratory for analysis such as separation through high performance liquid chromatography (HPLC)[12], ELISA[13], or via radioimmunoassay (RIA) kit[14], which can detect down to levels of pg/mL. Each of these techniques requires trained technicians in a clinical laboratory setting, expensive supplies and analysis equipment, and in the case of RIA, radioactive materials. Additionally, due to the sampling efforts and time needed for analysis, instant feedback of orexin A levels of the individual are not possible using these techniques. Real-time detection of biomarkers, such as orexin A, without time-consuming and labor-intensive laboratory analysis is a true need for multiple applications. Sensors using an electrical signal for transduction, such as the field effect transistor[15] (FET) and chemiresistor[16], have recently been studied for detecting a variety of molecules[17,18]. These sensors can be easily integrated into a modular chip design and programmed to sense a specific molecular target by functionalizing the semiconductor with a biorecognition element (BRE). The BRE is typically an antibody[19], DNA or RNA aptamer[20], or peptide[21] specifically selected and designed to bind the target of interest. The binding event changes the local electron density on the surface of the semiconductor resulting in a change in the current flowing through the device, signaling the presence of the target. In this work, we present a real-time electronic based sensor platform for detecting orexin A in biofluids at physiologically relevant concentrations.

2.0 RESULTS

We have developed an electronic based (FET) label-free biosensor with a novel integrated biological recognition element that provides real-time detection of orexin A in saliva and serum. The biological recognition element which binds orexin A was selected using a phage display technique, detailed in the methods section, and verified through both binding kinetics and computational modeling. The BRE is integrated into an electronic based sensor platform where the target binding event is reported discretely and rapidly (**Supplementary Fig. 1**).

2.1 Phage Display and Binding Kinetics

Candidate orexin A binding peptides (OABP) were obtained through phage display using the Ph.D. 12 phage display from New England BioLabs. Two sequences of interest, DQSNKIISLQRLGSG and TPWFQWHQWNLNGSG, referred to as OABP1 and OABP2 respectively, were identified. To accurately determine the binding kinetics of the peptide-orexin A complex, several concentrations of orexin A binding peptides were injected over a low-density surface of biotin-labeled orexin A immobilized on a streptavidin surface plasmon resonance (SPR) chip using a Biacore T-200. Kinetic fits of the OABP1 and OABP2 SPR sensorgrams (**Fig. 1**) indicates that OAPB1 binds with higher affinity than OABP2 (**Table 1**). From these rate constants, Kd is calculated as 74 +/- 2.1 nM for OABP1, which is comparable to the affinities determined from ELISA. As a negative control, the OABP1 sequence was randomized to QRQLNDKLSIISGSG (termed NCP) and tested for binding to orexin A, showing no binding (**Fig. 1**). OABP1 was tested for its ability to bind native protein in solution and used in a peptide pull down experiment in which it was bound to streptavidin magnetic beads and incubated overnight with 50 µM solutions of orexin A. The beads were washed extensively and the bound protein was eluted. Samples were run on a SDS-PAGE gel and detected by Western Blot with an anti-orexin A monoclonal antibody (**Supplementary Fig. 2**). Elution samples were split with half of the sample analyzed by silver stain and half analyzed by Western Blot. From the silver stained gel, it can be seen orexin A was precipitated along with one other prominent proteins from the sample. As a preliminary test of specificity in complex biological matrices, 200 ng to 1665 ng of orexin A was spiked into human brain cell lysate (1 mg/mL in 100 µl HBS-EP) and streptavidin beads coated with 1 µg /ml of OPB1 were used to pull down orexin A using the same PPD procedure and Western Blot protocol as described above with the exception that BSA was removed from the final wash buffer (**Supplementary Fig. 3**).

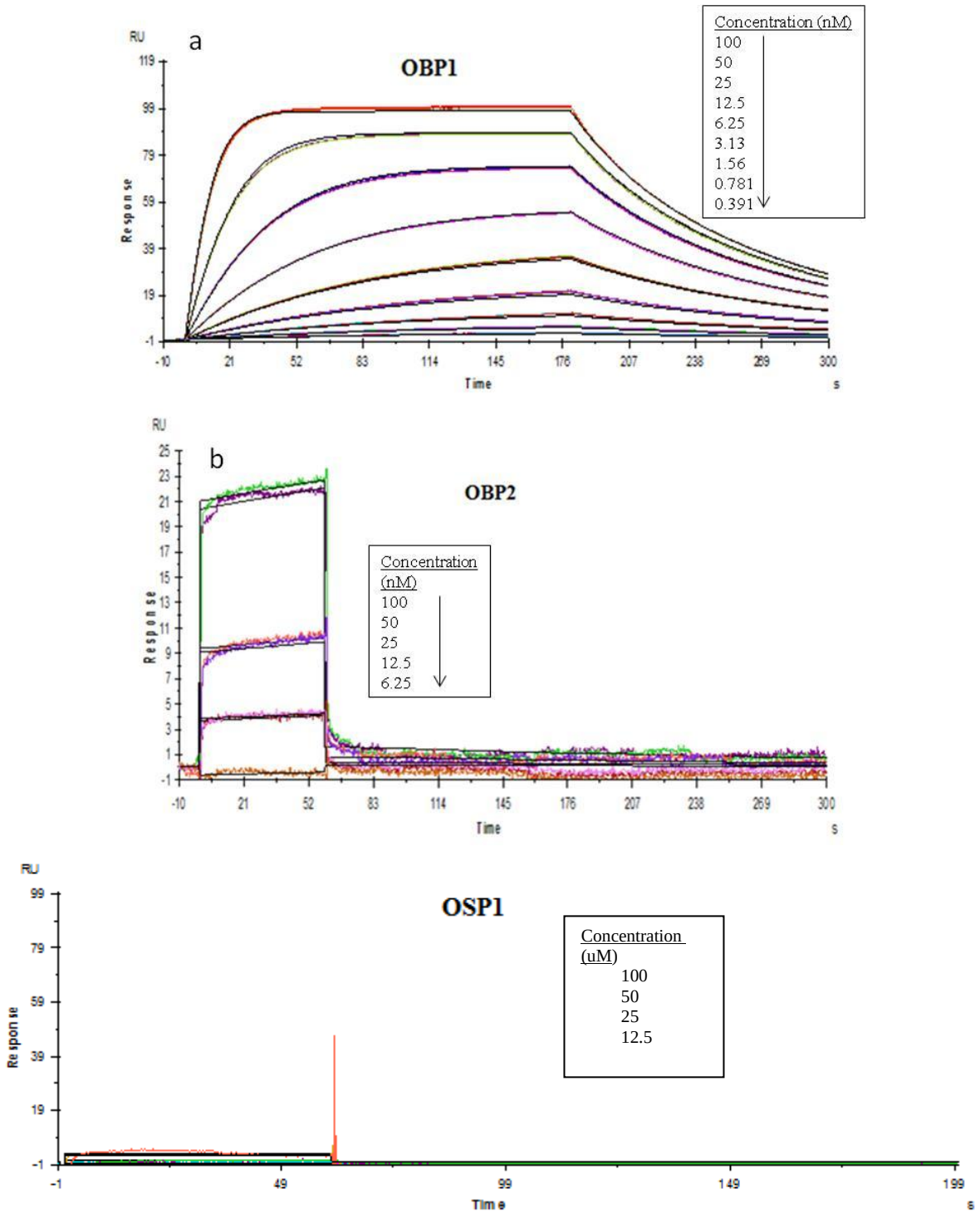

Figure 1. SPR sensorgrams and kinetic fits for OABP1, OABP2 and scrambled orexin A binding peptide (NCP)

Table 1. Equilibrium Dissociation Constants and kinetic Constants for orexin binding peptides. On-rates (Ka), off-rates (Kd) and dissociation constants (KD) shown were determined from kinetic fits of several sensorgrams across the same concentration series used in equilibrium binding response analysis.

Peptide	Sequence	Ka (1/Ms)	Kd (1/s)	KD
Orexin binding peptide (OABP1)	DQSNKIISLQRLGSG	2.62×10^5	0.0194	74±2.1nM
Orexin binding peptide (OABP2)	TPWFQWHQWNLNGSG	3.28×10^4	1.38	42±1.2µM
Scrambled orexin peptide (NCP)	QRQLNDKLSIISGSG	NB	NB	NB

2.2 Computational Modeling

Due to the higher binding affinity of OABP1, this peptide sequence was used for all computation modeling and sensor platform studies detailed in the remaining sections of this paper. The molecular modeling approach of characterizing the orexin A neuropeptide and binding peptide (OA-OABP1) interactions has two objectives. The first is to predict the three-dimensional arrangement of an OA-OABP1 complex given the known orexin-A three-dimensional structures[22]. The second objective is to estimate the OA-OABP1 binding energy. One of the most difficult problems in peptide-peptide docking is the flexibility of peptides which have many more degrees of freedom comparing with typical small molecules. To address this issue, a two-step process is typically used for predicting the structure of protein-protein complexes[23]. Initially, the proteins are considered as rigid molecules and a global search of the rotational and translational space is performed to generate a set of possible complexes. The second stage, called refinement, optimizes and rescores the generated rigid-body conformations by allowing small backbone and side-chain movements for both proteins[24]. We applied a similar approach to study the binding of peptides to the orexin A molecule. The rigid docking was performed by using the PatchDock package which is based on the molecular shape complementarity algorithm[25]. The generated structures were processed with the FireDock package for flexible docking[26]. FireDock performs refinement of each candidate complex by allowing side-chain flexibility and adjustment of the relative orientation of the molecules.

The experimental NMR structure of the orexin A molecule was retrieved from the Protein Data Bank (code 1WSO). Coordinates from the first NMR structure were used in computational docking. Figure 2a shows the unbound structure of orexin A. The residues drawn in red (Leu16, Leu19, Leu20, His26, Gly29, Ile30, Leu31, Thr32 and Leu33) correspond to residues which are involved in binding to orexin-1 receptor[27]. It was shown by Darker et al.[27] that replacement of these residues with alanine resulted in a significant drop in functional potency at the Ox1R receptor.

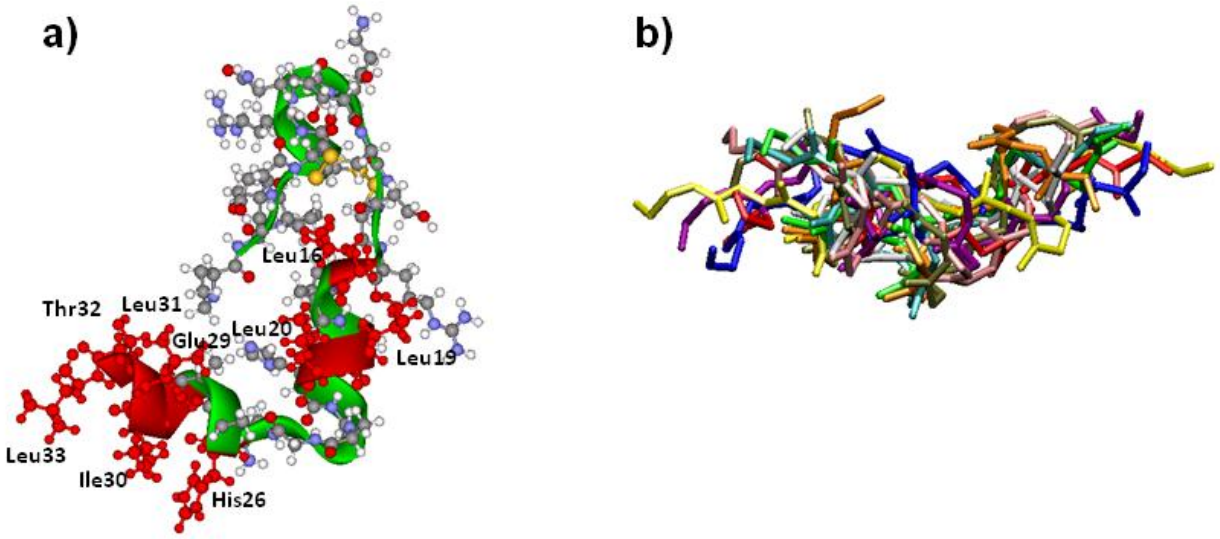

Figure 2. Unbound configurations of molecules used in docking
a) The experimental structure of orexin A[22]. The residues drawn in red are involved in binding to orexin-1 receptor. b) Ten representative unbound conformations for orexin A binding peptide (only backbone atoms are shown). Structures were visualized with Accelrys's Discovery Studio Visualizer (http://accelrys.com/products/discovery-studio/).

Short peptides, such as OABP1 and a negative control binding peptide (NCP) used in this study, are very flexible and often lack a well-defined conformation in their unbound state. Therefore, we generated an ensemble of unbound configurations for OABP1 and NCP using replica exchange molecular dynamics[28]. A total of 1000 generated conformations for each peptide were used in docking calculations. The representative ten unbound conformations for OABP1 are presented in **Figure 2b** (only backbone atoms are shown). The backbone atom root-mean square deviations were in the range of 1-5Å, which indicates a significant variability in peptide conformations.

The docking of binding peptides to orexin A was performed in two steps. Initially, the PatchDock package, that considers molecules as rigid, was used to perform a global search of the rotational and translational space based on shape complementary to the generated set of possible complexes. The generated structures were refined using the FireDock software for each candidate complex by allowing the side chains flexibility and adjustments of the relative orientation of the molecules. The refined complexes were scored and ranked according to FireDock energy function. **Figure 3** shows the highest ranked conformation of the OA-OABP1 complex. It can be easily seen that OABP1 peptide binds into the same region of the orexin A molecule as the Ox1R receptor through a combination of electrostatics, hydrogen bonding, and Van der Waals interactions. In the proposed structure of the complex, residue Leu12 is located at the side of orexin A molecule that allows it to link to the FET surface without the interruption of a complex. NCP also binds to the orexin A molecule although at a much lower level compared with the OAPB1 (**Table 2**).

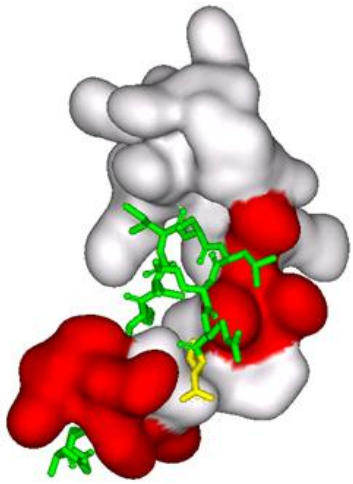

Figure 3. The proposed docking conformation of orexin A with OABP1
The binding peptide is presented as sticks on the surface of orexin A molecule. The part of orexin surface that corresponds to residues that are involved in binding to orexin-1 receptor is drawn in red. The residue Leu12 that forms a bond with G4 linker is drawn in yellow.

Table 2. Binding free energy for 5 top conformations of the OA-OABP1 and OA-NCP

Complex #	Binding Peptide		Negative control	
	ΔG (kcal/mol)	k_D	ΔG (kcal/mol)	k_D
1	-11.46	3.9 nM	-6.87	9.1 μM
2	-9.19	180 nM	-6.45	18.5 μM
3	- 6.12	32.3 μM	-4.51	500 μM
4	-2.73	10 mM	-2.77	9 mM
5	-2.08	30 mM	+0.14	-----

Initially, the docking configurations for orexin A with OABP1 and NCP were scored with the FireDock energy function[26]. That function takes into account atomic contact energy (ACE), van der Waals interactions, partial electrostatics, hydrogen and disulfide bonds, p-stacking and aliphatic interactions and additional terms[24]. Although the FireDock scoring function allows a ranking of binding complexes based on their binding affinity, it does not allow the calculation of the binding free energy.

Therefore, we refined the top predicted complex of orexin A with OABP1 using molecular dynamics (MD) simulations. We used the Amber10[29] package to perform MD simulations and the absolute binding free energy was calculated using the molecular mechanics/Poisson-Boltzmann surface area (MM/PBSA) methodology[30]: $\Delta G_{binding} = \langle G^{complex} \rangle - \langle G^{orexinA} \rangle - \langle G^{peptide} \rangle$. To prepare a system for MM/PBSA calculations, the OA-OABP1 complex was solvated in a rectangular box of TIP3P water molecules. The system was initially minimized to 1000 steps followed by 35 ps of equilibration at 300K with the restrain on all solute molecules. Next, we performed energy minimization for the entire system. Then, the system was equilibrated for 50 ps at 300K and, finally, we run a production run for 1 ns. The snapshots of the system trajectory were saved every 10 ps of MD simulations. These snapshots were used to extract the structure of the OA-OABP1 complex as well as unbound molecules. The entropic contribution was

calculated using a normal-mode analysis[31]. **Table 2** shows the binding free energy for the 5 top conformations of OA-OABP1 and OA-NCP. As the data indicates, complexes of OA-OABP1 have lower binding free energies that correspond to significantly higher binding affinity comparing to complexes of OA-NCP. The calculated dissociation constants K_D for the OA-OABP1 complexes are in the low pM to nM range, compared with low to high μM range for the OA-NCP complexes.

2.3 Sensor Development and Testing

The electronic sensor platform is based on a zinc oxide field effect transistor (ZnO-FET), which has several device and biosensor advantages. First, ZnO is deposited via pulsed laser deposition at room temperature conditions which lends to less expensive fabrication demands and ability to use a variety of substrates, including flexible and lightweight plastics[32]. Secondly, ZnO deposited under the correct conditions naturally forms a vertically aligned nanostructure giving the semiconductor enhanced surface area which is ideal for FET sensors. High performance ZnO FETs have been developed for high speed electronic applications[33] and also used as a sensor platform for small molecule liquid state sensing using a DNA aptamer as a BRE[34]. The selectivity of the system reported here is based on a bi-functional peptide designed to bind to both the ZnO[35] semiconductor as an anchor to the FET and to the biomarker target, orexin A. This anchor-sensor motif was successfully used in peptide BRE FETs based on carbon nanotubes[21] and graphene[36] for trinitrotoluene sensing. The ZnO FET structures are based on an interdigitated electrode design with a 2μm gap and back gate electrode (**Fig. 4a**). The device stack up is a doped Si wafer, SiO_2 insulator, ZnO semiconductor, and gold electrodes (from bottom up). The ZnO is etched (dark region in **Fig. 4a**) for confinement to the active electrode area and to keep each FET electrically isolated from its neighbor. The diced FET chips (15mm x 5mm) were incubated in the peptide solution for 6 minutes, washed and dried. A common approach for attaching BREs to surfaces is through covalent linker chemistry[37]. This approach is effective, although it can be difficult to control the density of linker and BRE densities on the surface, which directly affects sensor reproducibility. The anchoring peptide domain is based on the sequence

developed by Tomczak et al[35] which binds to ZnO. This sequence is added to the orexin A binding peptide (OABP1) sequence with a four glycine residue linker to provide flexibility and separation between the two domains, resulting in a sequence of DQSNKIISLQRL-GGGG-LHVMHKVAPPRGGGC (OABP1 – 4G linker – ZnO binder). The placement of the Leucine end of the OABP1 sequence to the 4G linker was specifically chosen based on the computational modeling data showing the importance of the amino acids on the Aspartic Acid end of OABP1 to the binding of orexin A. The bi-functional peptide approach is very effective in this design, with the ZnO anchor sequence preferentially binding to the semiconductor over any other surface on the FET array. This is shown in **Figure 4b** where the surface morphology of the SiO_2 region is completely flat (**Fig. 4a-ii**), whereas the ZnO region shows a large surface morphology change (**Fig. 4a-iii**) due to the attachment of the bifunctional peptide to the semiconductor. The functionalized ZnO PeptiFET maintains a high performance after processing with ON/OFF ratios of 10^8 and good current response with modulation of both the gate (V_G) and source/drain (V_{SD}) voltages (**Fig. 4c**).

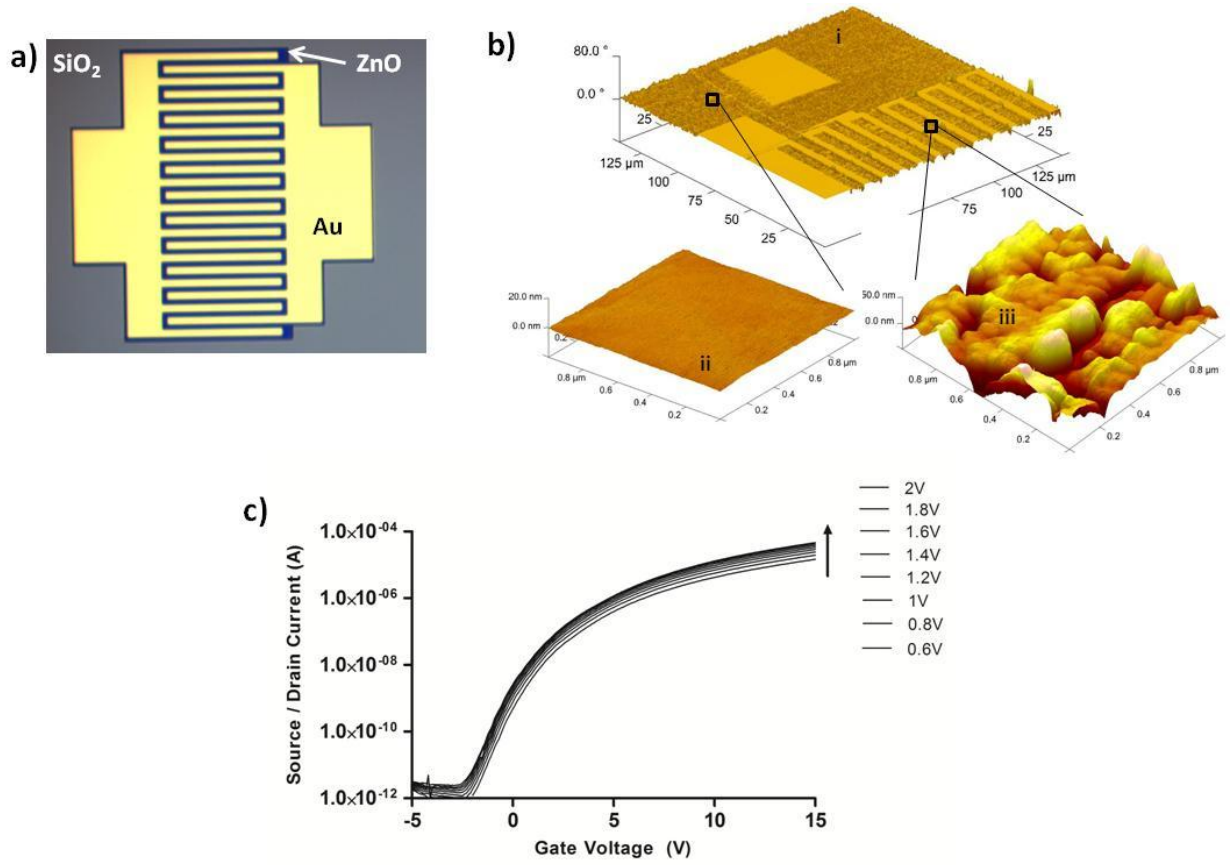

Figure 4. Attachment and dry state performance of the ZnO PeptiFET
a) *Optical micrograph of interdigitated electrode ZnO-FET structure.* ***b)*** *Atomic force micrographs of functionalized PeptiFET overall device structure (i), SiO_2 region morphology (ii), and ZnO region morphology.* ***c)*** *PeptiFET dry state performance with modulation of V_G and V_{SD}.*

Real-time sensor response was obtained by exposing the PeptiFET to various concentrations of orexin A target solutions while monitoring the source/drain current (I_{SD}) at a constant V_G and V_{SD}. For liquid state sensing, the PeptiFET must be rehydrated in order for effective binding of orexin A to take place. This is done by exposing the device to 20µL of water and monitoring the I_{SD} until it is stabilized. At this time, the sensor can be exposed to solutions containing the target or negative control molecules. The sensor was exposed to a solution containing 10 nM orexin A for 1 min and the source drain current was monitored. A rapid response in the current was observed that reaches a

plateau within 60 seconds. Orexin A has an overall positive charge (pI = 7.8), so the addition of a more positive charge distribution on the surface of the n-type semiconductor causes an increase in current upon binding. The sensor was exposed to varying concentrations of orexin A, (10 nM to 1 µM), and monitored over several minutes. Exposure of the sensor to increasing concentrations of orexin A also resulted in a concomitant increase in current (**Fig. 5a**). The magnitude of current increase at higher concentrations begins to decrease due to saturation of the peptide binding sites.

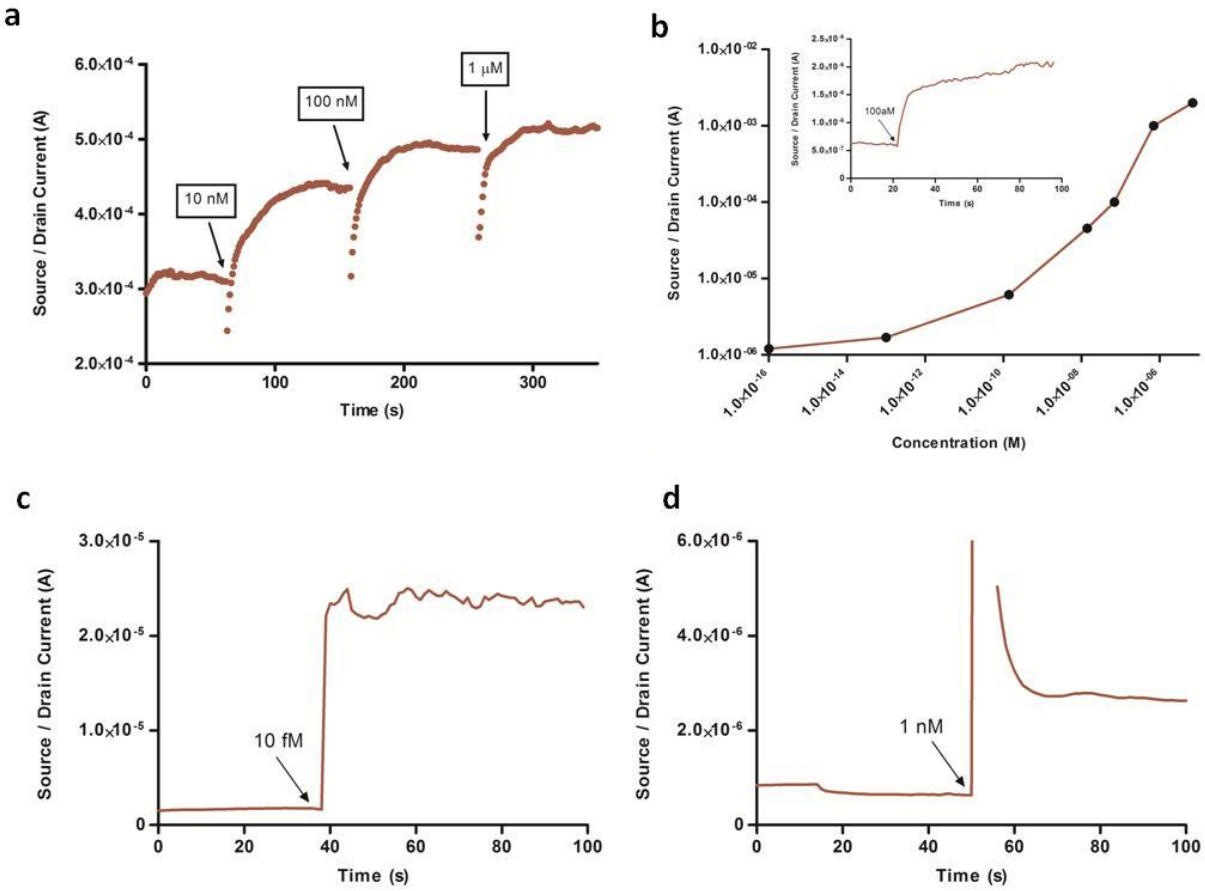

Figure 5. Real-time sensor response of the PeptiFET to orexin A
(a) *Increase in I_{SD} within multiple additions of orexin A at concentrations of 10 nM, 100 nM, and 1 µM for V_G = 5V and V_{SD} = 0.5V.* ***(b)*** *Sensitivity response of orexin A PeptiFET as overall current change versus concentration. Inset: maximum sensitivity real-time response to 100aM orexin A in water, for V_G = 5V and V_{SD} = 0.2V.* ***(c)*** *Real-time detection of 10 fM orexin A in saliva.* ***(d)*** *Real-time detection of 1 nM orexin A in fetal bovine serum.*

For these real-time static measurements, (single drop, no flow through) the response for each concentration of orexin A is determined by difference in current change from the stabilized rehydration step to the stabilized target exposure step. For a given V_G and V_{SD}, a response curve can be generated as overall increase in current (A) as a function of concentration of orexin A. This response curve is shown in **Figure 5b**, with the current change increasing with an increase in orexin A concentration, as expected. The overall sensitivity of this orexin A PeptiFET in water was determined at 100 aM ($1x10^{-16}$ M), which for the given volume added corresponds to ~1200 total molecules of orexin A (**Fig. 5b inset**).

2.4 Real-time detection in biological fluids

The response of the PeptiFET to orexin A in water is an important study for the proof of concept of the device scheme, but the ultimate application of this sensor is in the real-time detection in biological fluids such as saliva and serum, where sub-nM detection is needed[2,3,4,5,12,13]. Orexin A has a relatively low molecular weight (3561 g/mol) compared to many of the other molecules in the blood and saliva, such as blood cells, proteins, and enzymes. Therefore, a simple pre-processing step of size exclusion filtration using a 0.2 µm filter can be applied to both saliva and serum to lower the background noise of the biological fluid systems and increase the sensitivity on the PeptiFET. HPLC analysis of the biofluids before and after filtration show that the chemical composition of the samples were not altered (**Supplemental Fig. 5**). Before the filtration process, the sensitivity of the PeptiFET in a saliva matrix was seen at 1.4 µM (**Supplemental Fig. 6**). After filtration, the PeptiFET showed significant response to 10 fM ($1x10^{-14}$) of orexin A when spiked into a 20 µL drop of human saliva, as shown in **Figure 5c**. Likewise, the PeptiFET can detect down to 1 nM of orexin A when spiked in filtered fetal bovine serum (**Fig. 5d**). A rapid initial increase in the current is observed in the presence of orexin A followed by a stabilization period. The rapid increase is likely due to the initial disruption of charged species near the semiconductor surface after dropwise addition of the target solution.

Negative control experiments are essential to FET sensor evaluation since many semiconductor materials can show current response to a wide variety of molecules and environments. Orexin A tested on an unfunctionalized ZnO FET showed a negligible current change (**Supplemental Fig. 7**). Thus the effects of non-specific binding of the target to the FET are minimal. The BREs add specificity to the sensor, but must also be evaluated against negative control target molecules. Since orexin A is a 33 amino acid peptide, the most stringent negative control that can be tested is a peptide with the same 33 amino acids, but with a different sequence from that of native orexin A. Orexin A sequence was randomized with the following sequence: TGRLKLQCGALPICHQTPHALSLLEAYGRDCCN (MW = 3561, pI = 7.8), as compared to orexin A: QPLPDCCRQKTCSCRLYELLHGAGNHAAGILTL (MW = 3561, pI = 7.8). The randomized sequence is labeled as the negative control target (NCT). This molecule was exposed to the PeptiFET sensor at a concentration of 100 nM, where a slight increase in current ($2x10^{-7}$A) was detected (**Fig. 6a**). The same negative control peptide (NCP) used in binding kinetics and modeling (**Table 1**) was also used in the evaluation of the sensor performance. The following sequence was used: QRQLNDKLSIIS-GGGG-Z1 (NCP-Z1), where Z1 is the ZnO binding sequence, compared to the positive control: DQSNKIISLQRL-GGGG-Z1 (OABP1-Z1). In this case, 100 nM orexin A was exposed to a ZnO FET which was functionalized with NCP, again only a slight increase in current ($2x10^{-8}$A) was observed (**Fig. 6b**). However, when the negative control responses are overlaid with positive control responses (**Fig. 6c**), they become negligible. Direct comparison of 100 nM exposures shows an increase in signal of 115X over the negative control target, and 1,115X over the negative control binding peptide. Additionally, the response of the positive control PeptiFET to 100 aM orexin A is also overlaid in **Figure 6c**, also showing the minimization of negative control response in water. Similarly, minimal response was seen in negative control testing in saliva (**Supplemental Fig. 8**). The data obtained in the PeptiFET with the OABP1-Z1 (**Fig. 6b and 6c**) showed a ~1000x increase in signal over the PeptiFET functionalized with the NCP, corresponding with the ~1000x increase in K_D shown in **Table 2**.

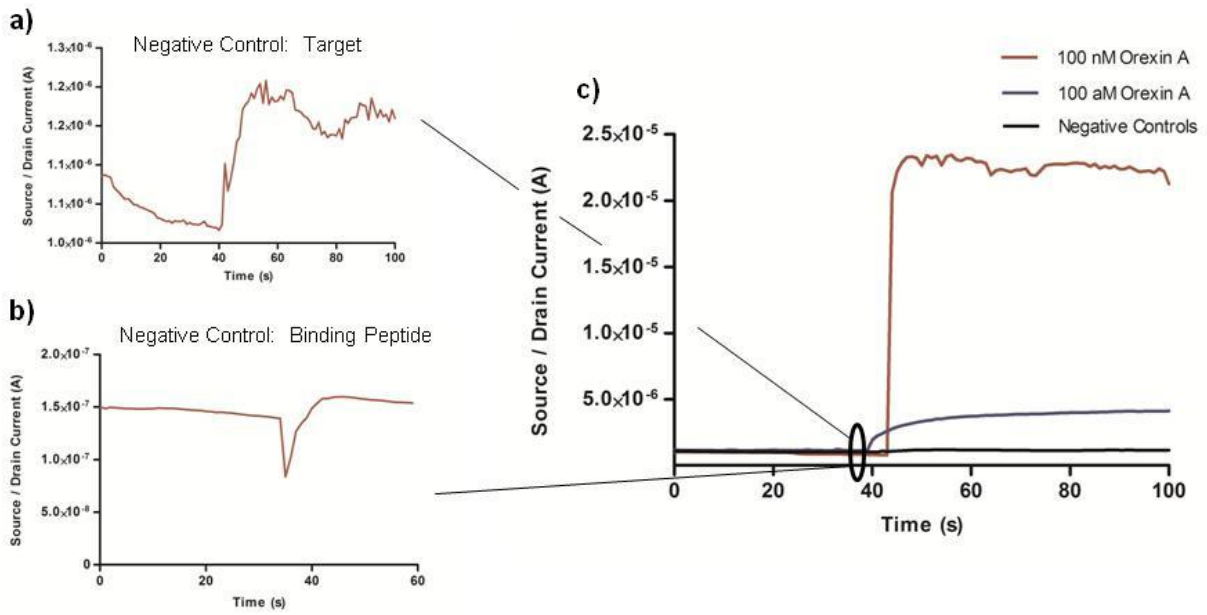

Figure 6. Negative control sensor testing
(a) *PeptiFET device functionalized with positive control binding peptide and exposed to negative control scrambled target peptide.* ***(b)*** *PeptiFET device functionalized with negative control scrambled binding peptide and exposed to 100 nM aqueous orexin A.* ***(c)*** *Overlay of positive and negative control real-time sensor response.*

3.0 DISCUSSION

Biomarker analysis in biofluids is a powerful tool for understanding the relationship between different types of events and the physiological and emotional state of a subject. Current methods to study biomarker levels involve timed intervals of biofluid sampling during a tasking, offline analysis, and data correlation after the fact. Studies are limited due to the inability to include rapid biofeedback in order to modify the tasks *in situ* or to provide any augmentation to counter the detrimental events. One example of a proposed augmentation is the intranasal administration of orexin A[6] when decreases in attentional performance are observed indicated by lower orexin A levels in the subject. Thus, we have developed a sensor platform approach to provide rapid biomarker analysis in biofluids.

Real-time biomarker sensing in biological fluids is complicated by the diversity and number of different molecules present in the biological fluids. An effective method to sensing in high background environments is by utilizing biological recognition elements (BRE), which are designed to selectively bind a target of interest. We report the evaluation of an experimentally selected and fully characterized **(Table 1)** binding peptide for the neuropeptide orexin A, which is a biomarker linked to fatigue and cognitive level[1,2,3,4,5]. Molecular modeling approaches were taken to further understand and characterize the interactions between the selected binding peptide and the neuropeptide orexin A. This is an important step in the design of BRE based sensing devices to optimize the system for maximum sensitivity and selectivity. For instance, since the binding peptide is tethered to a semiconductor surface, we must know which portion of the sequence is most involved in binding to make sure it is not hindered from binding. A two step process[23] was taken for this study involving rigid docking of the two peptide sequences using PatchDock[25] to generate a set of possible complex structures, followed by flexible docking of these structures via FireDock24. These experiments, along with a previous study of orexin A receptors show that the following amino acids are essential to the binding complex: Leu16, Leu19, Leu20, His26, Gly29, Ile30, Leu31, Thr32 and Leu33. The top binding complexes were ranked according to the FireDock scoring function and then refined and further analyzed using molecular dynamics simulations. Through these final simulations, the binding energy of the top scoring complexes was determined at levels of low pM to nM range, corresponding well to the sensor data. Additionally, the negative control binding peptide was analyzed the same manner, and showed a significant decrease in binding affinity of 1000X to high μM range, again correlating well to experimental values, where ~1000X greater signal was seen in positive control sensors over negative control.

This binding peptide was integrated into a field effect transistor (FET) structure where the binding of the target was transduced into an electrical signal. The advantages to this electrical based approach is (relative) ease of fabrication, ability of FETs to be highly arrayed, low power requirements (coin cell battery), and simple reporting that is amenable to wireless communication. This sensor architecture resulted in selective detection down to 100 aM concentrations in water (**Fig. 5b**), 10 fM in filtered human saliva

(**Fig. 5c**), and 1 nM in filtered fetal bovine serum (**Fig. 5d**). We have demonstrated the sensitivity and selectivity of the BRE by testing the sensor performance in complex fluids and using a variety of peptide controls.

We believe the sensor platform presented in this study can be used for analysis of a complex signature of biomarkers in multiple biofluids in real-time by arraying the FET elements and functionalizing each with a BRE specific to each biomarker, and applicable to a wide variety of neuroscience research applications.

4.0 MATERIALS AND METHODS

Peptides were custom synthesized and purchased from GenScript (New Jersey) and purified via HPLC to >95% purity with the following sequences:

Orexin A binding peptide + ZnO peptide (OABP1-Z1):

DQSNKIISLQRL-GGGG-LHVMHKVAPPRGGGC

Orexin A negative control binding peptide + ZnO peptide (NCP-Z1):

QRQLNDKLSIIS-GGGG-LHVMHKVAPPRGGGC

Target negative control (TNC):

QPLPDCCRQKTCSCRLYELLHGAGNHAAGILTL

Sterile water (UltraPure distilled DNAse RNAse free) was purchased from Invitrogen, orexin A (human, rat, mouse) was purchased from Sigma Aldrich and used without further purification, normal human saliva was purchased from Innovative Research (Novi, MI), and fetal bovine serum was purchased from Invitrogen. Saliva and serum were used either in the native state or filtered in a 0.2 µm PTFE syringe filter. ZnO FETs were fabricated on a doped Si substrate with a insulating layer of 30 nm SiO_2. ZnO was deposited on the insulator via pulsed laser deposition (PLD) at room temperature to a thickness of 100 nm, and patterned using photolithography and etching for electrical separation between FETs. Source/drain electrodes of titanium/platinum/gold (20/30/50 nm) were deposited by evaporation and liftoff techniques.

4.1 Peptide Selection: Phage Display

Panning procedures were conducted following the New England Biolabs Ph.D.-12 Kit protocol for micro scale phage selection and amplification. Orexin A target protein (150 µl) purchased from Sigma (10 nM orexin in 100 mM NaHO3, pH 8.6) was adsorbed on to the surface of the well in a 96-well microtiter plate. After an overnight incubation at 40 ºC, 200 µl of blocking buffer (100 mM NaHO3, 5 mg/ml BSA, pH 8.6) was added and incubated for 1 hour at 40 ºC. The blocking buffer was removed and the wells were washed six times with wash buffer (50 mM Tris-HCl (pH 7.5), 150 mM NaCl; TSB) at room temperature, then the phage library (approximately 6x1010 phage in TBS with 0.1 % Tween 20) was added to the well and mixed by gentle agitation. After incubation, the unbound phages were removed and the wells were washed 10 times with wash buffer. The bound phage were then eluted using 150 µl 200 mM glycine pH 2.2 (Aldrich) containing 0.5% BSA (Sigma) , rocked gently for 10 min at room temperature and neutralized using 15 µl of 1M Tris (Sigma) pH 9.1. The eluate was added to 20 mL E. coli ER2738 culture and incubated at 37 ºC with vigorous shaking for 4.5 h. The culture was transferred to a centrifuge tube and spun for 10 min at 10,000 x g at 40 ºC. The supernatant was collected and 1/6 volume of PEG/NaCl (20% PEG8000, 2.5 M NaCl) was added. The phage was allowed to precipitate at 40 ºC overnight. PEG precipitation was spun for 15 min at 10,000 g at 40 ºC. The pellet was re-suspended in 1 mL TBS, and re-precipitated with PEG/NaCl. Finally the pellet was suspended in 200 µL TBS, and stored at 40 ºC. The procedure was repeated 4 times for a total of 5 rounds of panning with the exception that the Tween concentration was increased 0.05% per round. Phage titers were determined as described in the Ph.D.-12 manual.

After five rounds of panning**,** 50 phage plaques were randomly selected from fresh titer plates using a sterile inoculation loops, and were amplified individually for 4.5-5 hours at 37 ºC in 1.5 mL of *E. coli* ER2738 culture grown in LB broth with 20 mg/L tetracycline (Sigma) until $O.D._{600}$ = 0.4-0.6. After incubation, the amplified plaque solutions were centrifuged twice (6,000 rpm, 10 min) and the supernatants were transferred to a sterile 1.5 mL microcentrifuge tubes. Phagemid DNA was then isolated from the purified phage stocks using the Qiagen QIAprep Spin M13 kit (Qiagen). DNA concentration and purity measurements were made using a Thermo Fisher Scientific NanoDrop™

spectrophotometer. DNA samples were then sent to The Ohio State University (http://pmgf.biosci.ohio-state.edu/index.html) for sequencing. The random 12 amino acid sequence (12-mer peptide) was determined by translating the DNA sequence.

4.2 Binding Peptide Characterization

Each orexin A peptide was synthesized by AnaSpec (Fremont, CA) with a mini PEG2-Lys-Biotin on the carboxy group. The synthesis scale was 2 µmole with > 98% purity. Lyophilized peptide was dissolved with molecular grade water at pH 7.4 to a concentration of 1 mg/ml. The peptides were further diluted to a ~0.1 mg/ml concentration in HBS-EP (10 mM HEPES pH 7.4, 150 mM NaCl, 50 mM EDTA, 0.005% (v/v) Surfactant P20 at pH 7.2), before being further diluted to give an SPR assay concentration of ~50 µg/ml. Orexin binding peptides, OABP 1 and 2 were synthesized by AnaSpec at the 2 umole scale with 98% purity. Orexin scrambled peptide QRQLNDKLSIISGSG (NCP) was used as a negative control.

Binding Kinetics. Surface Plasmon Resonance (SPR) experiments were done on a Biacore T200 SPR system (GE Healthcare, Piscataway, N.J.). All buffers and reagents were purchased from G.E. Healthcare unless otherwise noted. A standard coupling protocol was employed to immobilize a streptavidin capture surface as described by the manufacturer. The immobilization was performed at 25 °C using sodium acetate (10 mM in 150 mM NaCl, pH 4.5) as the running buffer. Biotinylated orexin A was flowed over flow cell 2 at10 µL/min until the desired level of capture was achieved (100RU), Flow cells 1 and 4 cells was used as a reference spots. Predicted Rmax values based on protein capture levels for all assays were kept within the range of 50-150 RU.

Data Analysis. Dissociation (Kd) and association (Ka) rate constants were obtained by nonlinear regression analysis of the primary sensorgram data according to a 1:1 binding model using the BiaEvaluation version 3.2 software provided by the manufacturer. The dissociation constant KD was calculated using the formula KD = kd / ka.

Binding Pull-Down Assays. Biotinylated orexin A peptide was immobilized onto prewashed streptavidin coated magnetic beads (DynaBeads M-280 streptavidin, Invitrogen, Carlsbad, CA) by incubating 1 µg of OABP1 with 25 µL of bead slurry at room temperature for 60 min. Beads without OABP1 were used as a control to evaluate nonspecific binding to the beads. A second control was conducted using human brain cell lysate (1mg/mL, ProSci Incorporated, Poway, CA) to assess the potential for the orexin A peptide to bind with proteins present in the lysate. Cell lysate components that bound nonspecifically to the beads were removed by incubating cell lysate (1mg/mL in 100 µL HBS-EP) with 50 µL of washed streptavidin beads and rotated at 40 ºC overnight. The next day, the magnetic beads were collected and the pre cleared cell lysate was removed and used in the pull-down experiments. OABP1 coated beads were washed five times with 500 µL of 1x HBS-EP supplemented with 0.1% BSA and incubated overnight at 40 ºC with rotation in the presence the desired amount of orexin A target protein (Sigma, St Louis, MO) in HBS-EP buffer with 0.5 mg of pre-cleared cell lysate. After binding, beads were washed five times with 500 µL of HBS-EP and heated at 70 ºC in 20 µL of Tricine sample buffer (BioRad, Hercules, CA) for 10 min. One half of each elution sample was analyzed by 10-20 % Tris-Tricine SDS-PAGE(BioRad) with 5-10 µL of Precision Plus protein dual Xtra strandard and Kalidoscope polypeptides markers (BioRad) for 45 min at 80 V and imaged after staining with the Silver SNAP staining kit (Pierce Thermo Scientific, Rockford, IL). The other half of the sample was analyzed by SDS-PAGE and the target was detected by using Western blot (SuperSignal West Dura, Pierce Thermo Scientific) with anti-goat orexin A antibody (C19, Santa Cruz Biotechnology, Inc.). The western blot was imaged on a GE Healthcare Typhoon Trio.

Affinity Determination by ELISA. Immunosorbant assays (ELISA) were conducted by incubating 1000 ng of orexin A protein in 0.1 M sodium bicarbonate, pH 9.8, in a Maxisorb NUNC 96-well plate overnight at 4 °C in a humidifier. The solution was removed and replaced with 100 µL of blocking buffer (2% BSA in PBS, pH 7.4), which was incubated for 1 h at 37 °C in the humidifier. The solution was removed, and the plate was washed three times with PBS-tween and tapped dry. The biotinylated OABP1 peptides were added to the plate at varying concentrations in PBS-tween (0.05%). The peptides were incubated

with the plate for 1 h at 37 °C. The solution was removed, and the plate was washed three times with PBS-tween. Horseradish peroxidase conjugated streptavidin was diluted 1:1000 in 0.1% BSA in PBS-tween, and 50 µL was added to each well and incubated for 1 h at 37 °C. The strepavidin solution was removed, and the plate was washed three times with buffer PBS-tween. Fifty µL of TMB (3,3′,5,5′-tetramethylbenzidine) was added to each well, and the solution was incubated for 15 min at 24 °C. Fifty µL of aliquot of 0.5 M HCl was added to stop the reaction, and the plate was scanned immediately using a SpectroMax plate reader. These assays were conducted in triplicate, and the data were then normalized by subtracting all fluorescent values from the no protein control, plotted, and fit using GraphPad Prism.

4.3 Sensor Platform: Equipment

Sensor device testing was done using a Keithley semiconductor parameter analyzer (SCS 4200) and MMR 4-probe station for addressing the FET source and drain electrodes. Atomic force microscopy images were taken with a Veeco BioScope AFM in tapping mode.

Functionalization

A 3” silicon wafer with a dense array of ZnO FETs was diced into ~15 mm x 5 mm FET arrays. These smaller arrays contain 6 FETs with identical geometries (**Fig. 4a**) which can each be tested individually. The bifunctional peptides were solubilized in UltraPure water at a concentration of 20 µg/mL and aliquotted into 1.5 mL sterile (autoclaved) plastic vials at a volume of 1 mL. The diced FET arrays were then incubated in the vial, gently shaken for 6 minutes, and immediately washed with UltraPure water and dried with nitrogen. Both the peptide concentration and incubation times were optimized for this sensor system. The peptide functionalized ZnO FET (PeptiFET) was then evaluated for sensor performance (preferably within 4 hours of functionalization).

4.4 Device Testing

The PeptiFET devices were tested in a real-time mode by applying a constant source/drain voltage (V_{SD}) and gate voltage (V_G) and monitoring the source/drain current (I_{SD}) at a rate of one data point per second. In order for effective target binding to take place, the binding peptide must be rehydrated. This was done by applying an initial 20 µL drop of UltraPure water and monitoring the current (I_{SD}) until stabilized (~2-3 minutes). When I_{SD} reached a stable value, the target solutions were applied and sensor performance analyzed.

4.5 Modeling

In our computational study, we used the 3D structure of orexin A determined using a two-dimensional nuclear magnetic resonance (NMR) spectroscopy and posted into the Protein Data Bank (PDB code 1WSO)[22]. The structures of OABP1 were generated using the Rosetta *ab initio* fragment assembly package[38]. The 1000 top-scoring structural models were refined by energy minimization, rescored with an implicit solvent model, and clustered by a pairwise hierarchical method to identify a set of unique structures using a protein structure prediction pipeline (PSPP)[39]. To account for the peptide flexibility, an ensemble docking technique was applied. The models with the lowest energy in ten clusters as predicted by PSPP were selected as input structures for replica exchange molecular dynamics (REMD) simulations[40].

The REMD simulations were performed with the Amber10[29] suite of programs as implemented in Automatic Protein Ensemble Generator (https://applications.bioanalysis.org/apeg). Eight replicas distributed over a temperature range from 270 to 600 K were used. The implicit water simulations for each replica were initially equilibrated for 200 ps at the corresponding temperature following by 5 ns of production run. The time step was set to 2 fs and SHAKE was applied to constrain the bonds connecting hydrogen atoms. The temperature exchanges were attempted every 1 ps and 5000 snapshots from the production run were used for cluster analysis. Clustering was performed with the Amber10 PTRAJ modules based on the pairwise backbone-atom only root-mean square deviations (RMSD). Saved snapshot

conformations were clustered into 100 clusters and representatives from each cluster were taken for docking. A total of 1000 cluster representatives obtained for 10 conformations generated by Rosetta were used in docking calculations.

The OA-OABP1 docking was performed in two steps. The rigid docking was performed using the PatchDock package[25] with the default set of parameters. The generated structures were processed to the FireDock package[26] for flexible docking. The refinement procedure was performed in three steps. Initially, we performed a coarse refinement using the restricted interface side-chain optimization (RISCO) mode with an atomic radii scaling of 0.8 and a 50 cycles of Monte Carlo rigid-body optimization (RBO). Next, the 25 best configurations were processed for a fine refinement using the full side-chain optimization (FISCO) mode, an atomic radii scaling of 0.8 and a 50 cycles of RBO. Finally, the top 10 models were selected for a full-side optimization with the radii scaling of 0.85 but without RBO. The refined complexes were scored and ranked according to FireDock energy function.

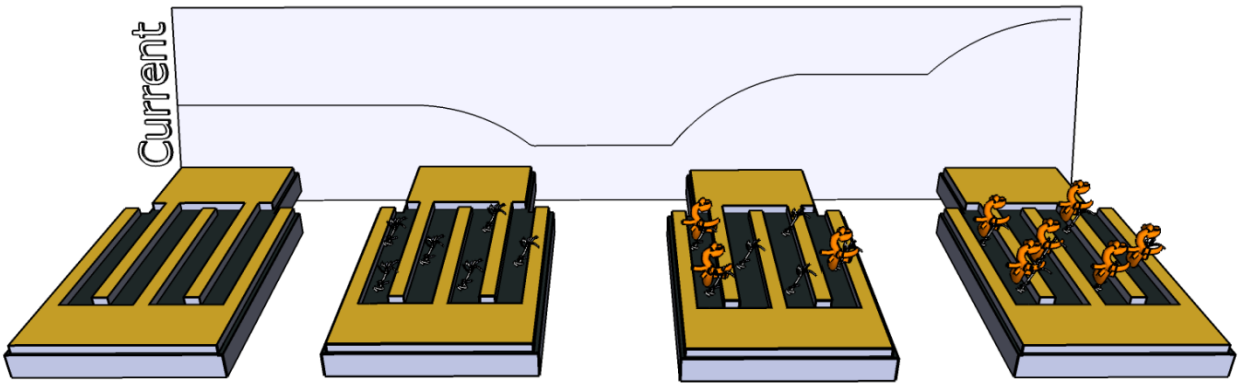

Supplemental Figure 1. Overall schematic of sensing platform (L to R): Bare zinc oxide field effect transistor, ZnO FET functionalized with binding peptide (PeptiFET), PeptiFET exposed to low concentration of Orexin A then bound to the binding peptide, higher concentration of Orexin A added to PeptiFET. Signal representation shows the trend of real-time current response during each step.

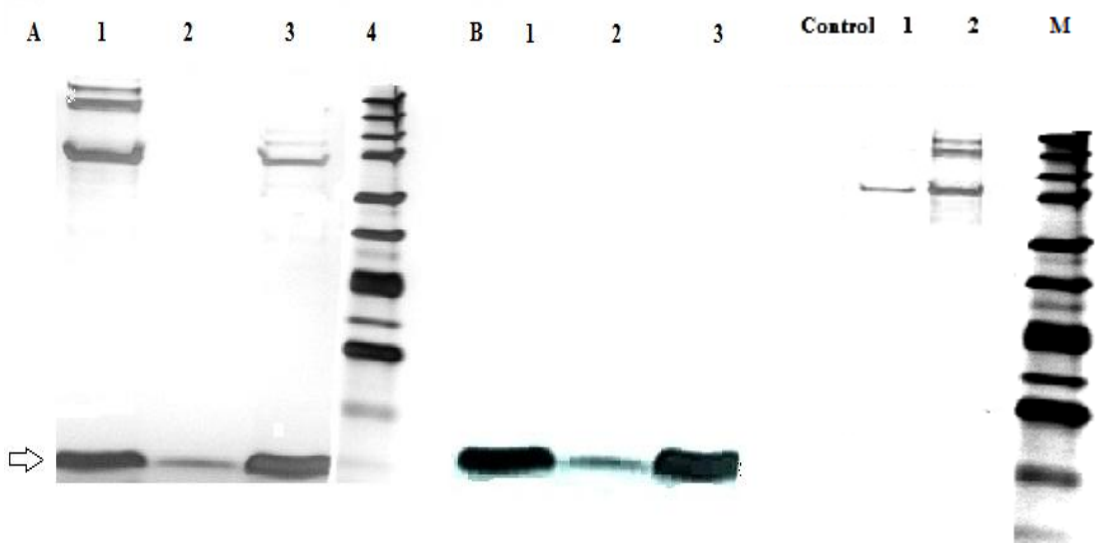

Supplemental Figure 2. SDS –PAGE analysis of OABP1 pull down assays. A) Lane 1: Silver stain gel image of the final eluted fraction from the orexin A pull down was performed with immobilized OABP1 in the presence of excess brain cell lysate (1 mg/ml).

Lane 2: Purified 10 µl of 25 µM orexin A solution was used as the control. Lane 3: orexin A pull down performed with immobilized OABP1 in the presence of buffer without brain cell lysate. The arrow marks the orexin A band which shows efficient removal of orexin A from buffer and buffer/brain cell lysate solutions by the OABP1 peptide. Lane 4 Marker: Precision Plus protein dual Xtra strandard and Kalidoscope polypeptides markers (BioRad). One band in appear in both pull downs assays and were attributed to background bead binding due to wash buffer components. B) The band at the bottom of the gel marked with an arrow was validated as orexin A with a Western Blot. C. Control experiments are as follows: lane 1: beads loaded with peptides and lane 2 beads loaded with peptides and spiked with cleared brain lysate.

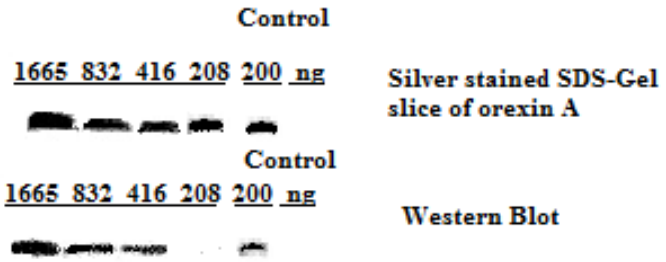

Supplemental Figure 3. OABP1 pull down assays. A) Lane 1: Silver stain gel image of the final eluted fraction from the orexin A pull down assays (1665-200 ng of orexin A in each pull drop assay) was performed with immobilized OABP1 in the presence of excess brain cell lysate (1 mg/ml). 200ng orexin A solution was used as the control.

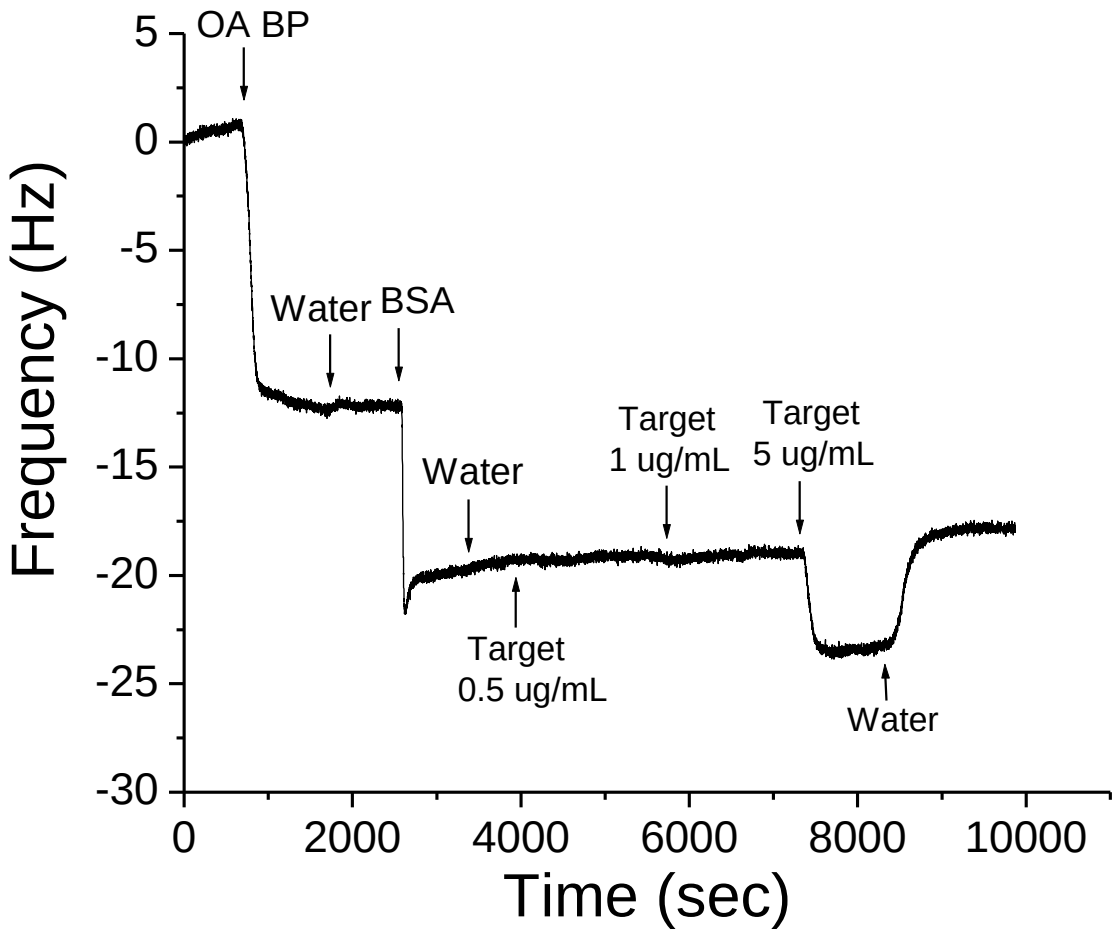

Supplemental Figure 4. Quartz crystal micrograph data (QCM) showing binding of Orexin A in water to the selected binding peptide. Biotinylated OABP1 was dissolved into sterile water and immobilized onto a streptavidin coated QCM crystal. Native orexin A was flowed over the functionalized crystal with flowrates shown above.

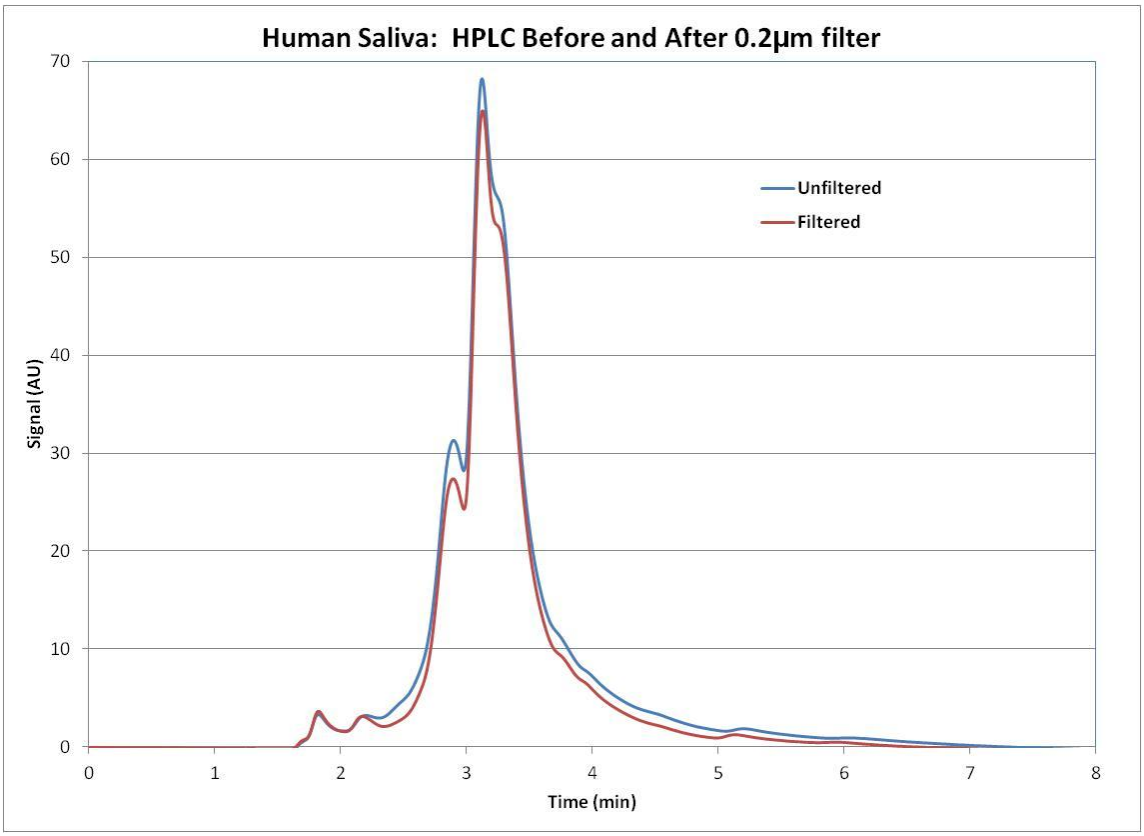

Supplemental Figure 5. HPLC analysis of human saliva unfiltered and filtered with 0.2 µm PTFE syringe filter.

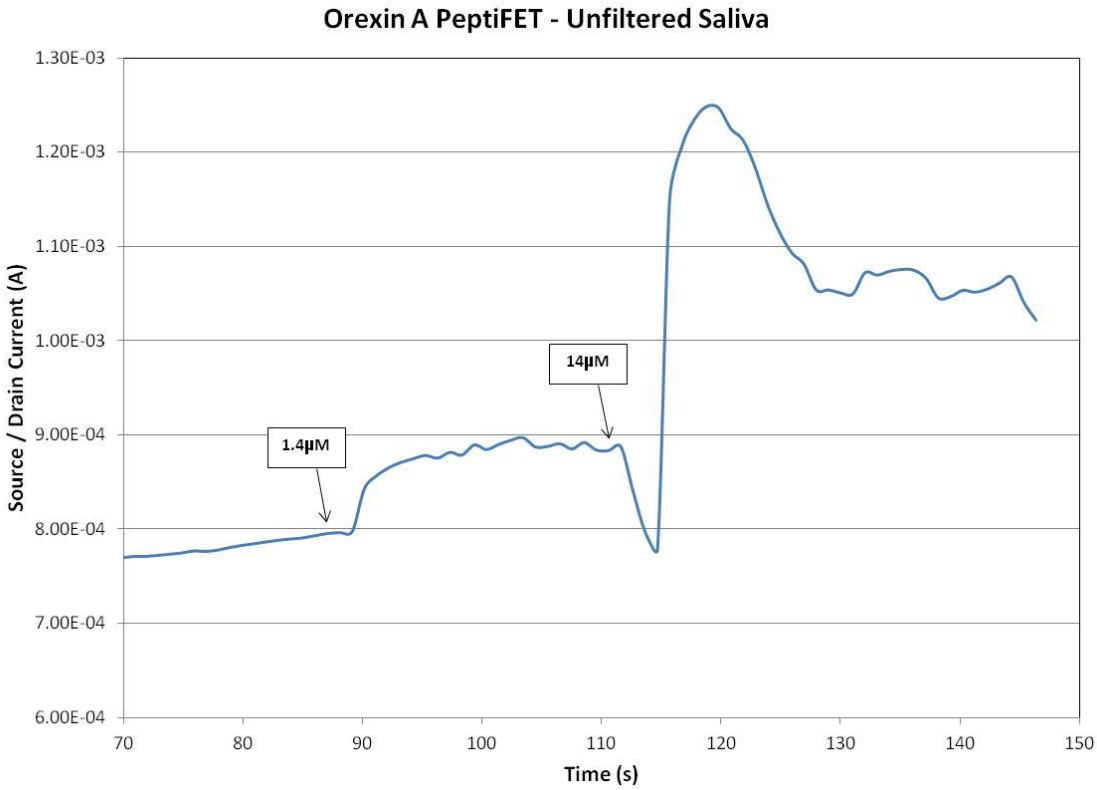

Supplemental Figure 6. Real-Time sensing of orexin A in pure human saliva. Addition of 1.4 µM (90 s) and 14 µM (110 s) of orexin A onto a saturated surface of unprocessed saliva.

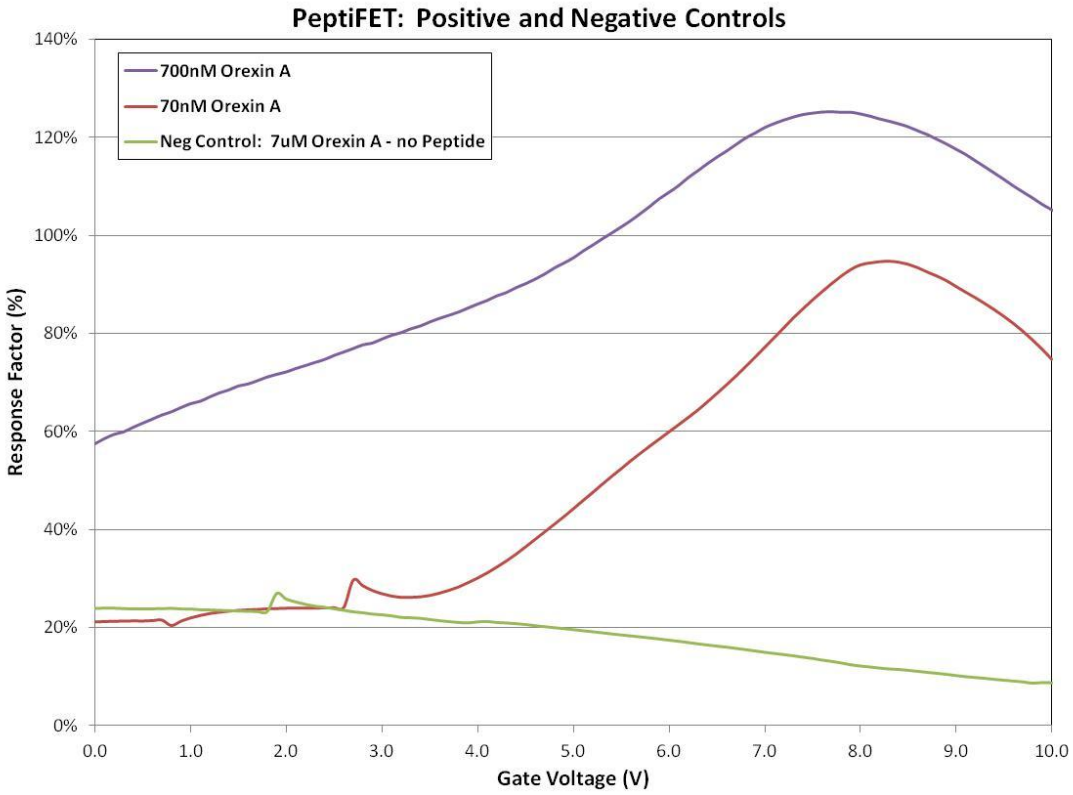

Supplemental Figure 7. Negative control – exposure of unfunctionalized FET to orexin A (green), with positive controls of 70 nM (red) and 700 nM (purple) overlayed. For these experiments, the gate voltage was modulated from 0-10V with a constant source-drain voltage of 0.5V. Response factor is based on current value before and after addition of target (I_{after}/I_{before}*100)

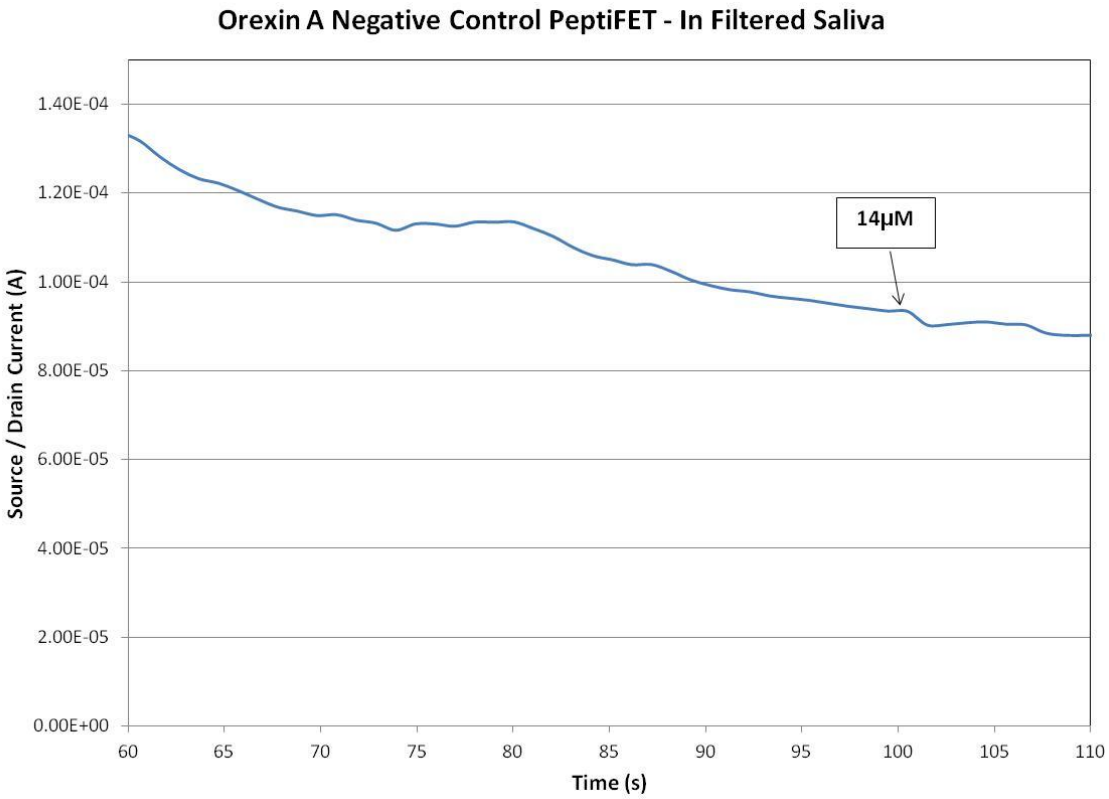

Supplemental Figure 8. Negative control – exposure of PeptiFET to negative control target in a matrix of filtered human saliva. Addition of 14 µM (100 s) of negative control orexin A onto a saturated surface of filtered saliva.

REFERENCES

[1] N. Tsujino & T. Sakurai, Orexin/hypocretin: a neuropeptide at the interface of sleep, energy homeostasis, and reward system. *Pharmacological Reviews* **61**, 162–176, (2009).

[2] Yoshida Y., Fujiki N., Nakajima T., Ripley B., Matsumura H., Yoneda H., Mignot E., & Nishino S. Fluctuation of extracellular hypocretin-1 (orexin A) levels in the rat in relation to the light-dark cycle and sleep-wake activities. *Eur J Neurosci* **14**, 1075–1081 (2001).

[3] Peyron C. *et al*. A mutation in a case of early onset narcolepsy and a generalized absence of hypocretin peptides in human narcoleptic brains. *Nat. Med.* **6**, 991–997 (2000).

[4] Higuchi S. *et al*. Plasma orexin-A is lower in patients with narcolepsy. *Neurosci. Lett.* **318**, 61–64 (2002).

[5] Strawn J., Pyne-Geithman G., Ekhator N., Horn P., Uhde T., Shutter L., Baker D. & Geracioti T. Low cerebrospinal fluid and plasma orexin-A (hypocretin-1) concentrations in combat-related posttraumatic stress disorder. *Psychoneuroendocrinology* **35**, 1001-1007 (2010).

[6] Deadwyler S.A., Porrino L., Siegel J.M. &Hampson R.E. Systemic and nasal delivery of orexin-A (hypocretin-1) reduces the effects of sleep deprivation on cognitive performance in nonhuman primates. *J Neurosci.* **27**, 14239–14247 (2007).

[7] Boschen K.E., Fadel J.R. &Burk J.A. Systemic and intrabasalis administration of the orexin-1 receptor antagonist, SB-334867, disrupts attentional performance in rats. *Psychopharmacology* **206**, 205–213 (2009).

[8] Sakurai T. *et al*. Orexins and orexin receptors: a family of hypothalamic neuropeptides and G protein-coupled receptors that regulate feeding behavior. *Cell* **92**, 573–585 (1998).

[9] Baranowska, B., Wolinska, E., Martynska, W., Chmielowska, M. & Baranowska-Bik, A. Plasma orexin A, orexin B, leptin, neuropeptide Y (NPY) and insulin in obese women. *Neuroendocrinology Letters* **26**, 293-296 (2005).

[10] Kastin, A. J., & Akerstrom, V. Orexin A but not orexin B rapidly enters brain from blood by simple diffusion. *J. Pharmacol. Exp. Ther.* **289**, 219– 223 (1999).

[11] Ammoun S., Holmqvist T., Shariatmadari R., Oonk H.B., Detheux M., Parmentier M., Akerman K.E., & Kukkonen J.P. Distinct recognition of OX1 and OX2 receptors by orexin peptides. *J Pharmacol. Exp. Ther.* **305**, 507–514 (2003).

[12] Arihara Z., Takahashi K., Murakami O., Totsune K., Sone M. & Satoh F. Immunoreactive orexin-A in human plasma. *Peptides* **22**, 139-142 (2001).

[13] Heinonen, M.V., Purhonen, A.K., Miettinen, P., Pääkkönen, M., Pirinen, E., Alhava, E. Åkerman, Herzig, K.H. Apelin, orexin-A and leptin plasma levels in morbid obesity and effect of gastric banding, *Regulatory Peptides* **130**, 7-13 (2005).

[14] Abdo W., Bloem B., Kremer H., Lammers G., Verbeek M., & Overeem. CSF hypocretin-1 levels are normal in multiple-system atrophy. *Parkinsonism and Related Disorders* **14**, 342-344 (2008).

[15] Patolsky, F. &Lieber, C. Nanowire nanosensors. *Materials Today* **8,** 20 (2005).

[16] Aswal, D., & Gupta, S. *Science and Technology of Chemiresistor Gas Sensors*, (Nova Science Publishers 2007).

[17] Cui, Y., Wei, Q., Park, H. & Lieber, C. Highly sensitive and selective detection of biological and chemical species. *Science* **293**, 1289-1292 (2001).

[18] Covington, J., Gardner, J., Briand, D. & de Rooij, N. A polymer gate FET sensor array for detecting organic vapours. *Sensors and Actuators B: Chemical* **77,** 155-162 (2001).

[19] North, J. Immunosensors: Antibody-based biosensors. *Trends in Biotechnology* **3**, 180-186 (1985).

[20] Maehashi, K., Katsura, T., Kerman, K., Takamura, Y., Matsumoto, K., & Tamiya, E. Label-free protein biosensor based on aptamer-modified carbon nanotube field effect transistors. *Anal. Chem*. **79**, 782-787 (2007).

[21] Kuang, Z. Kim, S., Crookes-Goodson, W., Farmer, B. & Naik, R. Biomimetic Chemosensor: Designing Peptide Recognition Elements for Surface Functionalization of Carbon Nanotube Field Effect Transistors. *ACS Nano* **4**, 452- 458 (2010).

[22] Takai, T. Takaya, T., Nakano, M., Akutsu, H., Nakagawa. A., Aimoto, S., Nagai, K. & Ikegami, T. Orexin-A is composed of a highly conserved C-terminal and a specific, hydrophilic N-terminal region, revealing the structural basis of specific recognition by the orexin-1 receptor. *J. Pept. Sci.* **12**, 443–454 (2006).

[23] Bonvin A.M. Flexible protein–protein docking. *Curr Opin Struct Biol* **16**, 194–200 (2006).

[24] Andrusier N., Mashiach E., Nussinov R. & Wolfson H.J. Principles of flexible protein–protein docking. *Proteins* **73**, 271–289 (2008).

[25] Duhovny, D., Nussinov, R. & Wolfson, H.J. Efficient unbound docking of rigid molecules *Proceedings of the Fourth International Workshop on Algorithms in Bioinformatics*, *September 17–21, 2002, Springer-Verlag GmbH Rome, Italy* **2452**, 185–200 (2002).

[26] N. Andrusier, R. Nussinov & H. J. Wolfson. FireDock: Fast Interaction Refinement in Molecular Docking. *Proteins*, **69**, 139-159 (2007).

[27] Darker J.G., Porter R.A., Eggleston D.S., Smart D., Brough S.J., Sabido-David C., Jerman J.C. Structure-activity analysis of truncated orexin-A analogues at the orexin-1 receptor. *Bioorg. Med. Chem. Lett.* **11**, 737–740 (2001).

[28] Sugita Y. & Okamoto Y. Replica-exchange molecular dynamics method for protein folding. *Chemical Physics Letters.* **314**, 141–151 (1999).

[29] Case, D. A. *et al*. *AMBER 10*, (University of California, San Francisco 2008).

[30] Kollman, P. A. *et al*. Calculating structures and free energies of complex molecules: Combining molecular mechanics and continuum models. *Acc. Chem. Res*. **33**, 889−897 (2000).

[31] Kottalam, J. & Case, D.A. Langevin modes of macromolecules: application to crambin and DNA hexamers. *Biopolymers* **29,** 1409-1421 (1990).

[32] Nomura, K. Ohta,H., Takagi, A., Kamiya, T., Hirano, M. & Hosono, H. Room-Temperature fabrication of transparent flexible thin-film transistors using amorphous oxide semiconductors. *Nature*, **432**, 488-492 (2004).

[33] Bayraktaroglu, B., Leedy, K. &Neidhard, R. High-frequency ZnO thin-film transistors on Si substrates. *IEEE Electron Device Letters* **30**, 946-948 (2009).

[34] Hagen J., Kim S., Bayraktaroglu B., Leedy, K., Chavez, J., Kelley-Loughnane N., Naik R., & Stone M. *Sensors* **11**, 6645-6655 (2010).

[35] Tomczak M., Gupta M., Drummy L., Rozenzhak S. & Naik, R. Morphological control and assembly of zinc oxide using a biotemplate. *Acta Biomaterialia* **5,** 876-882 (2009).

[36] Cui, Y., Kim, S.N., Jones, S.E., Wissler, L.L., Naik, R.R., and McAlpine, M.C. Chemical Functionalization of Graphene Enabled by Phage Displayed Peptides. *Nano Lett*. 2010, **10,** 4559–4565 (2010)

[37] Hermanson, G. *Bioconjugate Techniques* (Elsevier, New York 2008).

[38] Simons K.T., Kooperberg C., Huang E., Baker D. Assembly of protein tertiary structures from fragments with similar local sequences using simulated annealing and Bayesian scoring functions. *J Mol Biol.* **268**, 209–225 (1997).

[39] Lee M.S., Bondugula R., Desai V., Zavaljevski N., Yeh I.C., Wallqvist A. & Reifman J. PSPP: a protein structure prediction pipeline for computing clusters. *PLoS One* **4**, 6254 (2009).

[40] Sugita Y. & Okamoto Y. Replica-exchange molecular dynamics method for protein folding. *Chemical Physics Letters.* **314**, 141–151 (1999).